Effect of Nitrogen Ion Implantation on the Localized Corrosion Behavior of Titanium Modified Type 316L Stainless Steel in Simulated Body Fluid

T. Sundararajan, U. Kamachi Mudali, K.G.M. Nair, S. Rajeswari, and M. Subbaiyan

(Submitted 24 December 1997; in revised form 16 November 1998)

Nitrogen ion implantation on titanium-modified type 316L stainless steel (SS) at the energy of 70 keV was carried out at different doses ranging from 1×10^{15} to 2.5×10^{17} ions/cm^2. These samples were subjected to open circuit potential (OCP)—time measurement, cyclic polarization, and accelerated leaching studies—in order to discover the optimum dose that can provide good localized corrosion resistance in a simulated body fluid condition. The results showed that the localized corrosion resistance improved with an increase in doses up to 1×10^{17} ions/cm^2, beyond which it started to deteriorate. The results of the accelerated leaching studies showed that the leaching of the major alloying elements was arrested upon nitrogen ion implantation. Gracing incidence x-ray diffraction studies showed the formation of chromium nitrides at a dose of 2.5×10^{17} ions/cm^2. X-ray photoelectron spectroscopy studies revealed the presence of these chromium nitrides in the passive film, which was attributed to the decreased corrosion resistance at a higher dose. Secondary ion mass spectroscopy studies on the passive film showed the variation in the depth profile upon nitrogen ion implantation. Thus, nitrogen ion implantation can be effectively used as a method to improve the corrosion resistance of the orthopedic implant devices made of titanium-modified type 316L SS. The nature of the passive film and its influence on corrosion resistance are discussed in this article.

Keywords austenitic stainless steels, nitrogen ion implantation, passive film, pitting corrosion, titanium addition

1. Introduction

Inherent mechanical properties and corrosion resistance of metallic materials have necessitated their use as orthopedic implants for a long time. The austenitic stainless steels, especially type 316L stainless steels (SS), are the most popular because of their relative lower cost compared to cobalt-chromium and titanium and its alloys. They have reasonable corrosion resistance (Ref 1). However, it was reported that type 316L stainless steel orthopedic implants corrode in the human body environment and release chromium, iron, and nickel ions (Ref 2, 3). The failure of stainless steel implant devices (Ref 4-6) have revealed that the material cannot be used for a long period in a body fluid environment. Localized corrosion attack is caused mostly by failure; pitting and crevice corrosion were the most frequently observed types of localized corrosion attack. This demanded the need to look for alternate materials that possess good corrosion resistance. Addition of nitrogen as an alloying element to type 316L SS has been reported to significantly improve the localized corrosion resistance and decrease the release of major alloying elements during accelerated leaching studies in simulated body fluid (Ref 3). Altering the material by surface modification without affecting the bulk properties is an alternate way to increase the corrosion resistance. Ion implantation as a technique to improve the corrosion resistance of various materials has been widely studied (Ref 7, 8).

Nitrogen ion implantation is widely regarded as an effective process for the enhancement of aqueous corrosion resistance of various steels (Ref 7-9) because the beneficial effects of nitrogen addition on the localized corrosion resistance of austenitic stainless steels have been well established through bulk alloying (Ref 10, 11). However, the results of the electrochemical studies on nitrogen ion implanted austenitic stainless steel are often contradictory (Ref 12-14). The reason for the deterioration in corrosion resistance upon nitrogen implantation was attributed to the defects generated, the precipitates developed, and the phase transformation that occurred during ion implantation.

In the present investigation, a systematic study was made on titanium-modified 316L SS to determine the suitability of the

T. Sundararajan, S. Rajeswari, and **M. Subbaiyan,** Department of Analytical Chemistry, University of Madras, Guindy Campus, Chennai-600 025, India; and **U. Kamachi Mudali** and **K.G.M. Nair,** Metallurgy and Materials Group, Indira Gandhi Centre for Atomic Research, Kalpakkam-603 102, India.

Table 1 Elemental composition of 316L SS and titanium-modified type 316L SS

	Composition, %									
Specimen	**C**	**Si**	**Mn**	**Cr**	**Ni**	**Mo**	**Ti**	**S**	**P**	**Fe**
316L SS	0.025	0.98	1.76	17.9	12.1	2.45	…	0.002	0.02	bal
Ti 316L SS	0.024	0.61	0.81	15.4	14.7	2.4	0.21	0.006	0.03	bal

material for its application and their performance with nitrogen ion implantation. The optimum corrosion resistance of a nitrogen ion implanted specimen was evaluated using electrochemical techniques, namely, open circuit potential (OCP) - time measurements, potentiodynamic anodic polarization, and accelerated leaching studies. Gracing incidence x-ray diffraction (GIXD), x-ray photoelectron spectroscopy (XPS), and secondary ion mass spectroscopy (SIMS) studies have been attempted to understand the mechanism for variation in the corrosion parameters.

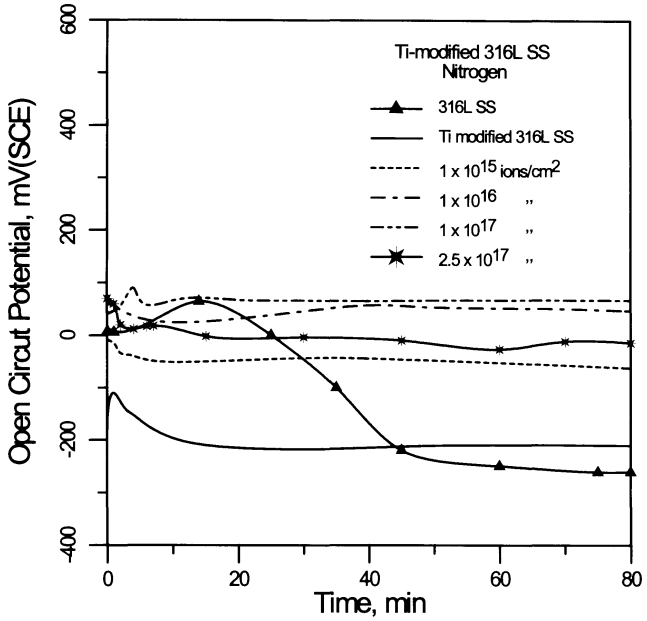

Fig. 1 Open circuit potential-time measurements on nitrogen ion implanted, titanium-modified type 316L SS specimens in comparison with unimplanted titanium-modified 316L and 316L SS

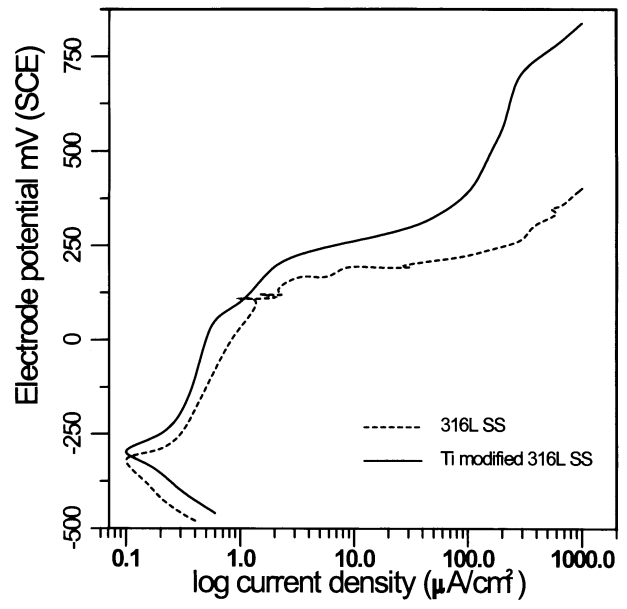

Fig. 2 Potentiodynamic polarization studies on unimplanted titanium-modified 316L SS reference to 316L SS in Ringer's solution

2. Experimental Procedures

Titanium-modified type 316L SS samples (Table 1), 8.5 mm diameter and 3 mm thick, were mounted using epoxy resin, polished with 1000 grit SiC paper, and then polished with 5 and 1 μm diamond paste. The samples were degreased with trichloroethylene and acetone followed by ultrasonic cleaning with deionized water. A type 316L SS specimen was also tested for comparison.

Nitrogen ion was implanted at a fixed energy of 70 keV for different doses, namely 1×10^{15}, 1×10^{16}, 1×10^{17}, and 2.5×10^{17} ions/cm^2. The vacuum was below 1×10^{-6} mbar at the target chamber during implantation.

Cyclic polarization studies of the implanted and unimplanted samples were carried out in Ringer's solution (9 g/L NaCl, 0.43 g/L KCl, 0.2 g/l $NaHCO_3$, 0.24 g/L $CaCl_2$) at pH 7.4 and a temperature of 37.4 ±1 °C. The potentials were measured using saturated calomel electrode (SCE) as a reference and platinum as a counter electrode.

The initial OCP of the samples immersed in the electrolyte was noted and monitored as a function of time until the samples reached a stable potential. Cyclic polarization experiments were conducted with a Wenking ST 72 potentiostat (Germany) coupled with a programmable scanner. When the samples attained a constant potential, cyclic polarization was started with an initial potential of 250 mV below the corrosion potential (E_{corr}). It was scanned in the positive direction at a sweep rate of 10 mV/min. The potential at which there was a monotonic increase in the current density in the passive region beyond 25 μA was defined as the pitting potential. Further scanning was continued until the current density of the specimen reached 1 μA, and then the scan was reversed back in the cathodic direction. Accelerated leaching studies were carried out in all the implanted samples by applying 100 mVfor 1 h in the previously mentioned solution. The major elements like iron, chromium, and nickel leached into the test solution were quantitatively analyzed in all the implanted specimens using atomic absorption spectroscopy.

The unimplanted and implanted (dose of 1×10^{17} ions/cm^2) specimens were passivated for XPS and SIMS analysis by keeping them at the potential of 100 mV for 1 h in Ringer's solution. After the immersion, the specimens were removed and kept in inert atmosphere before being transferred to the respective chambers.

3. Results and Discussion

Figure 1 shows the OCP- time measurement of nitrogen ion implanted titanium-modified 316L SS in comparison with unimplanted specimens of 316L SS and titanium-modified 316L SS. The OCP of the reference 316L SS showed a higher potential at the initial stage and subsequently fell to a low value of –260 mV at the end of 80 min. Titanium-modified 316L SS also behaved in the similar manner; it started with the initial potential of –100 mV and attained a constant potential of –210 mV in 25 min.

The nitrogen ion implanted, titanium-modified 316L SS attained a stable potential in a short duration with the shift in the

OCP toward a noble direction compared to the unimplanted specimen. The OCP of the implanted specimen increased with an increase in the dose up to 1×10^{17} ions/cm^2. Beyond this dose the OCP shifted to the negative direction for the specimen implanted at the dose of 2.5×10^{17} ions/cm^2. The shift in the OCP of these implanted specimens may arise from the noble surface layers produced by ion implantation (Ref 15).

Figure 2 shows the potentiodynamic polarization curves for unimplanted titanium-modified 316L SS in comparison with the unimplanted 316L SS. The pitting potential of 316L SS was +190 mV, and that of titanium-modified type 316L SS was +280 mV. This indicates the improved localized corrosion resistance of titanium-modified type 316L SS. A decrease in the current density at the passive region was also noticed for titanium-modified 316L SS compared to 316L SS.

Figure 3 shows the XPS Ti 2p spectrum for 316L SS and titanium-modified 316L SS in their passivated condition. The passive film of 316L SS does not show any peak at this region, whereas titanium-modified 316L SS showed a doublet at this region. These deconvoluted peaks present at 458.8 and 464.6 eV correspond for Ti $2p_{3/2}$ and $2p_{1/2}$ of TiO_2, respectively (Ref 16). This indicates the presence of titanium as its oxide in the passive film.

Many investigations have reported the improved localized corrosion resistance of titanium-added stainless steels (Ref 17-19). Titanium was considered to be helpful in forming TiS inclusions that are insoluble in acids in comparison with MnS inclusions (Ref 19). Inclusions of MnS are the most probable pit initiation sites, and they allow the early stage of pitting attack in the material. Avoiding these inclusions by forming TiS will enhance the localized corrosion resistance of the material (Ref 18). However, in the present investigation, XPS results showed the presence of titanium in the passive film, as oxides would have played a role in stabilizing the passive film. It was proposed (Ref 17) that titanium could play the following role in stabilizing the passive film in improving the pitting corrosion resistance: On anodic polarization, titanium also dissolves along with other alloying elements such as chromium, iron, nickel, and molybdenum and gets into the chromium-rich mixed oxide passive film. In general, the passive film of stainless steels has high concentrations of defects with bound water. The competition of adsorption between the oxygen and chloride ions from the electrolyte onto the passive film surface is the underlying mechanism of passivity (Ref 20). Pitting is initiated by the specific adsorption of chloride ions favored over oxygen ions. The presence of titanium in the passive film may reduce the defect concentration by occupying the vacant sites. Also, the absorption of oxygen ions will be favored by the titanium in the passive film, in preference to chloride ions. Titanium is also well known for binding vacancies and thus will impede the mobility of the ions across the film (Ref 21). The passive current density of titanium-modified 316L SS tended to show lower value than type 316L SS, indicating that the passive film was stabilized with the addition of titanium.

Figure 4 shows the potentiodynamic polarization curves for nitrogen ion implanted titanium-modified 316L SS specimens in comparison with the unimplanted specimen. The implanted specimens showed an improvement in the pitting potential (Table 2) with an increase in the dose up to 1×10^{17} ions/cm^2. Particularly, the specimen implanted at 1×10^{17} ions/cm^2 showed the highest value in pitting potential of +730 mV, which was more than a two-fold increase compared to pristine titanium-modified type 316L SS (+280). The specimen implanted at the dose of 2.5×10^{17} ions/cm^2 did not show any further improvement, and indeed it showed inferior pitting potential (+620) compared to the specimen implanted at 1×10^{17} ions/cm^2. This

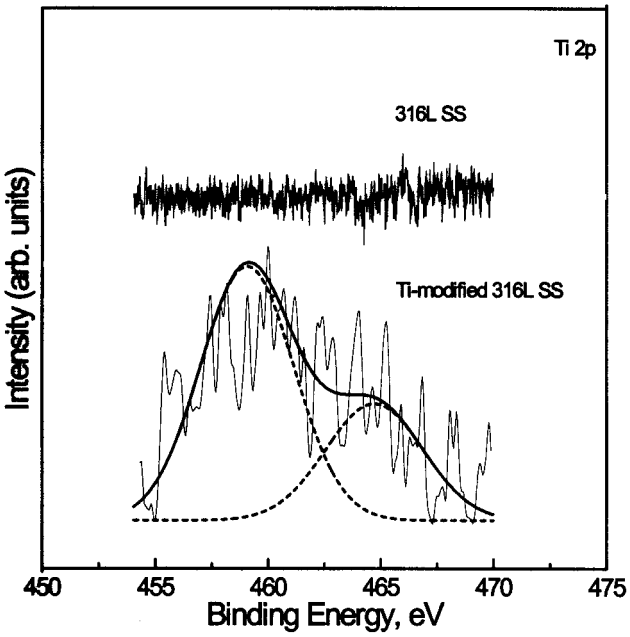

Fig. 3 X-ray photoelectron spectroscopy Ti 2p spectra for 316L SS and titanium-modified 316L SS specimens in unimplanted-passivated condition

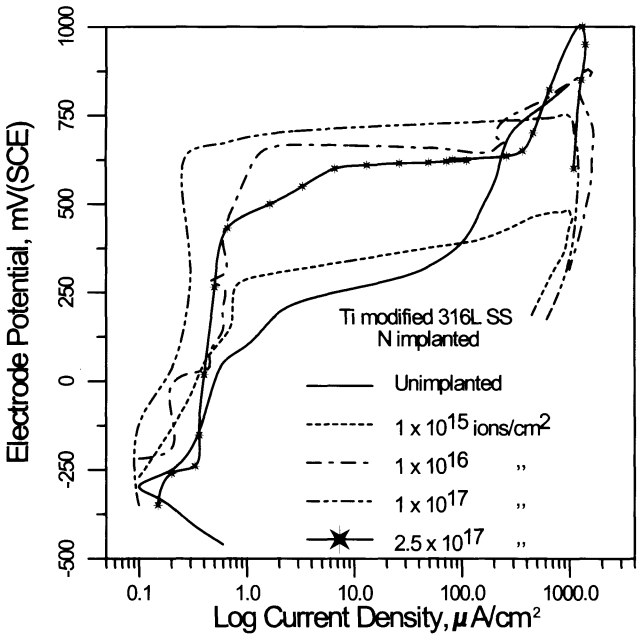

Fig. 4 Potentiodynamic polarization studies on nitrogen ion implanted titanium-modified type 316L SS at different doses compared to the unimplanted specimen

revealed that the high dose implantation (>1×10^{17} ions/cm^2) on titanium-modified 316L SS was not beneficial with respect to localized corrosion. The enhanced pitting resistance in the implanted specimens clearly indicated the beneficial effect of nitrogen ion implantation on titanium-modified 316L SS in a simulated body fluid condition.

In the accelerated leaching study, the concentration of the metal ions, such as iron, chromium, and nickel, present in the test solution after aging for 1 h was determined (Fig. 5). The results concurred with the result of OCP- time measurements and potentiodynamic polarization. A significant amount of metal ions was released into the solution for the unimplanted specimen, whereas the metal ion release started to decrease with an increase in the dose up to 1×10^{17} ions/cm^2. The increases in the amount of ions leached out at the dose of 2.5×10^{17} ions/cm^2 revealed the inhomogeneity in the passive film. Under in vivo conditions, the metal ions released from the implants were transported to the remote tissues through body fluids. It induced cytotoxic and allergic reactions and caused cancer (Ref 22). The minimization in the dissolution of the specimen implanted at the dose of 1×10^{17} ions/cm^2 revealed the enhanced stability of the passive film. There was no nickel found in the previously mentioned dose, which would be due to the enrichment of chromium, molybdenum, and nickel in the passive film.

The influence of nitrogen addition on the corrosion behavior of stainless steels through ion implantation was unclear. There was no improvement in the localized corrosion of nitrogen ion implanted 304 and 304L SS, which has been reported often (Ref 12-14), although the beneficial effect of nitrogen on the localized corrosion resistance of the previously mentioned materials has been well established through bulk alloying (Ref 10, 11). The detrimental effect was attributed to the defects generated, the precipitates developed, and the phase transformation during ion implantation. A study of the nitrogen ion implanted 304L SS by Marcus and Bussell (Ref 13) in the acid medium showed the increased current density in the passive region. The increased current density was attributed to the formation of chromium nitride during implantation, which would have remained as islands in the passive film. The inhomogeneities present in the passive film led to the increased passive current density.

Nair et al. (Ref 14) observed a decrease in the pitting potential of nitrogen ion implanted 304 specimens. The dose they chose for implantation was 1×10^{17} to 5×10^{17} ions/cm^2 at the energy of 30 keV. The implanted specimens showed no improvement in the localized corrosion resistance upon nitrogen implantation. The decrease in the corrosion resistance was attributed to the migration of chromium toward the grain boundaries forming chromium-rich ferrite phases in the austenitic structure, leaving the chromium depleted zones in the adjacent region.

It is interesting to note that in this study the dose chosen was 1×10^{15} ions/cm^2, and it showed a gradual improvement in corrosion resistance with an increase in the dose. The improvement in the corrosion resistance observed in this study was approximately at 1×10^{17} ions/cm^2 (70 keV), and above this dose a decrease in the corrosion resistance was observed. Also, the study from Leito et al. (Ref 15) showed the improvement in the corrosion resistance of 316L SS upon nitrogen ion implantation in Hank's solution, and the corrosion parameters varied with variation in the fluence of ion implantation. A high dose became detrimental in the electrochemical point of view.

Kamachi Mudali et al. (Ref 23, 24) also reported significant improvements in the pitting and intergranular corrosion resistance of nitrogen ion implanted sensitized 304 and 316 SS in acidic chloride medium. Several other investigations have also showed that nitrogen ion implantation improved the localized corrosion resistance on various steels (Ref 7-9). From the summary of the previously mentioned results, the following questions arose: (a) Why was the decrease in localized corrosion resistance noticed at higher doses for this alloy? (b) What is the mechanism by which nitrogen ion implantation improves the localized corrosion resistance on titanium-modified 316L SS? Surface characterization of the modified materials and their passive films were carried out to answer these questions.

3.1 Gracing Incidence X-Ray Diffraction Studies

Gracing incidence x-ray diffraction studies were carried out for the specimens implanted at 1×10^{17} and 2.5×10^{17} ions/cm^2 in comparison with an unimplanted specimen in order to explain the dependence of the corrosion resistance on the nitrogen fluence (Fig. 6). The unimplanted specimen also

Table 2 Corrosion parameters of 316L SS and titanium-modified type 316L SS

Specimen	Open circuit potential , mV	Pitting potential (Epp), mV	Passive current density ipass at 0 mV
316L SS	–261	+190	0.80
Ti modified 316 SS	–211	+280	0.50
N – 1×10^{15} ions/cm^2	–60	+350	0.35
N – 1×10^{16} ions/cm^2	+46	+670	0.23
N – 1×10^{17} ions/cm^2	+66	+730	0.16
N – 2.5×10^{17} ions/cm^2	–15	+620	0.40

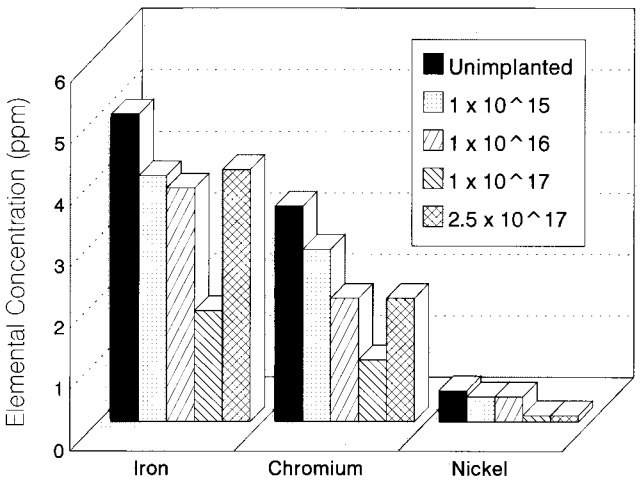

Fig. 5 Leaching pattern of alloying elements for nitrogen ion implanted specimens in comparison with unimplanted titanium-modified type 316L SS in Ringer's solution

showed the distinct peaks at the 2Θ value of 43.7 and 50.8. The peaks at 43.7 corresponded to the austenitic phase γ (111), and the peak at 50.8 was assigned to γ (200). Figure 5 shows the diffraction pattern of the specimens. The specimen implanted at the dose of 1×10^{17} ions/cm^2 showed a pattern similar to that of unimplanted specimens with an extra peak at the 2Θ values of 42.5. The peak at 42.5 with the *d*-spacing value of 2.11 corresponds to generation of martensite phase (α′). On the other hand, the specimen implanted at the dose of 2.5×10^{17} ions/cm^2 showed two additional peaks at 42.4 and 41.4, compared to the unimplanted specimen, which were responsible for α′ and Cr_2N respectively. This indicated that the nitrides have not formed at the dose of 1×10^{17} ions/cm^2, and the implanted nitrogen would have occupied the interstitial sites. The partial transformation of austenitic to martensite was observed at this dose. However, for the specimen implanted at the dose of 2.5×10^{17}, the intensity of the martensite was decreased with the formation of chromium nitride (Ref 21).

Vardiman and Singer (Ref 25) studied the nitrogen ion implanted 304 SS using secondary ion mass spectrometry, which showed that both CrN^+ and Cr_2N^+ were formed in preference to iron nitrides. Ion fluences were between 10^{16} and 10^{18} ions/cm^2 (40 keV). The CrN^+ yield increased linearly with nitrogen implant fluence, while Cr_2N^+ yield saturated at about 2×10^{17} ions/cm^2, the fluence at which the implanted nitrogen exceeds the chromium content. However in the present study, there were no nitrides of chromium found at the dose of 1×10^{17} ions/cm^2, although the energy was high compared to the study by Vardiman and Singer (Ref 25). This may have been due to less chromium content in the alloy (15.4%) compared to 304 SS where chromium content was about 18%. Whitton et al. (Ref 26) studied the phase transformation and compound formation in single crystal austenitic stainless steel by different fluence of nitrogen ion implantation. The results show that martensite formation was the precursor for the chromium nitrides formation. Leutenecker et al. (Ref 27) studied the kinetics of austenitic to martensite transformation and chromium nitride formation in AISI 321 SS. The results show that at room temperature implantation the partial martensite transformation has been observed with partial retaining austenitic at the dose of 1×10^{17} ions/cm^2. In higher doses (4×10^{17} ions/cm^2) the martensite phase was released by forming chromium nitride, whereas increasing the sample temperature condition or an increase in the beam current of the martensite transformation was still present. The martensite can develop by stress induced ion implantation. The reconversion of $\alpha' \rightarrow \gamma$ in competition with nitride was mostly caused by nitrogen saturation over the α′ stability limit; that is, generally at room temperatures (RT) after termination of chromium nitride. In this study the implantation was carried out at room temperature, and the beam current was maintained at 2 μA. The model described by Leutenecker et al. (Ref 27) perfectly fit the results of this study.

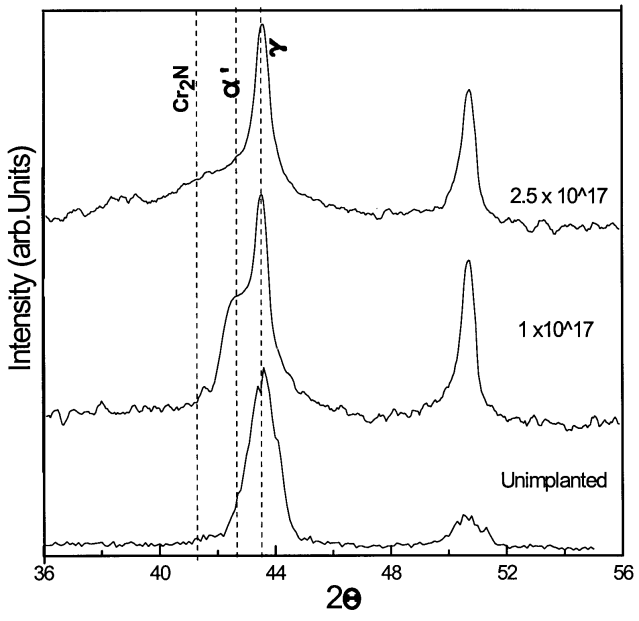

Fig. 6 Gracing incidence x-ray diffraction pattern of unimplanted and nitrogen ion implanted, titanium-modified type 316L SS

3.2 X-Ray Photoelectron Spectroscopy Studies

Figure 7(a) shows the Cr 2p spectrum of nitrogen ion implanted-passivated specimens of optimum dose (1×10^{17} ions/cm^2) and high dose (2.5×10^{17} ions/cm^2) specimens. The spectrum for optimum dose specimen showed a doublet at 576.6 and 581.3 eV corresponding to $2p_{3/2}$ and $2p_{1/2}$ peaks of Cr_2O_3 (Ref 28). The spectrum for high dose specimen showed the shift in the lower binding energy region, and this can be deconvoluted into four peaks. The peaks at 576.7 and 581.5 eV were assigned for $2p_{3/2}$ and $2p_{1/2}$ peaks of Cr_2O_3. The extra peaks at 565.5 and 579.0 eV were attributed to $2p_{3/2}$ and $2p_{1/2}$ peaks of CrN (Ref 29).

Figure 7(b) shows the N 1s spectra for the previous specimens with the same conditions. The implanted-passivated specimen of optimum dose showed a broad peak, which can be deconvoluted into three peaks. The peaks at 398.3, 400, and 403.5 eV were attributed, respectively, to nitrogen present in the solid solution, oxynitrides, and formation of nitrate during the anodic dissolution. In the high dose specimen, the peak shifted into the lower binding energy side, and in deconvolution it showed three peaks at 396.7, 398.7, and 400.2 eV. These peaks corresponded, respectively, to nitrides of chromium and nitrogen present in the interstitial and oxynitrides formation in the passive film (Ref 13, 30).

The GIXD and XPS results revealed that for implantation up to 1×10^{17} ions/cm^2, implanted nitrogen present in the interstitial and during the polarization studies converted into oxynitrides and inhibiting nitrate compounds. However, the appearance of chromium nitride was noticed in the specimen implanted with the dose of 2.5×10^{17} ions/cm^2, and it remained in the passive film. Marcus and Bussell (Ref 13) also found the chromium nitride in the passive film of nitrogen ion implanted 304L SS in the acidic medium, and decreased corrosion resistance of the implanted specimen was attributed to the nitrides. The decreased corrosion resistance of specimen implanted with 2.5×10^{17} ions/cm^2 was due to these precipitates, which created the adjacent chromium depleted zones. This led to the inhomogeneities in the passive film and made it a more pit probable site.

3.3 Secondary Ion Mass Spectroscopy Studies

Figure 8 shows the SIMS depth profile of pristine as-implanted, unimplanted-passivated, and implanted-passivated specimens. The pristine specimen (Fig. 8a) showed the high intensity of alloying elements (iron, chromium, nickel, molybdenum, and titanium) at the top layers toward the surface, as it reached the steady state including oxygen. Presence of oxygen at high intensity in the surface would have arisen from the oxide, particularly an air-formed oxide film. In the as-implanted specimen (Fig. 8b), oxygen showed the similar profile of a pristine specimen, whereas there was a distinct difference in the profile of alloying elements that showed a decreased intensity at the initial stage in the passive film, and it rapidly increased when it reached the bulk. The void was observed for all alloying elements in the implanted region, beyond which it attained a steady state. This may have been due to nitrogen incorporation in the region leading to diffusion of alloying elements into the bulk. In the oxygen profile, the increase in the depth of oxygen observed before attaining a steady state indicated that the thickness of the air-formed oxide film was higher for the as-implanted specimen compared to the pristine specimen. The increase in the OCP of the implanted specimens can be attributed to the air-formed oxide film, which increased the thickness with an increase in the duration of implantation. Ashworth et al. (Ref 31) found the increase in OCP of iron upon ion implantation, and it was attributed to the increase in the thickness of the air-formed oxide film. From this investigation, it was clearly shown that the thickening of the air-formed oxide film in the implanted specimen caused an increase in the OCP. However, in the specimen implanted at 2.5×10^{17} ions/cm^2, the OCP shifted toward active direction and may have arisen from the surface chemical changes produced due to high dose implantation.

The unimplanted-passivated specimen showed the similar profile of the pristine specimen except the change in the nickel and oxygen. In the case of nickel, there was a decrease in the intensity at the surface layers, and it increased with depth, indicating the least role in the passive film. In the oxygen profile the presence of oxygen was high toward depth compared to the pristine specimen. This reveals the increase in the thickness of the passive film upon potential impression.

The depth profile of implanted-passivated specimen did not show any major difference in the alloying elements compared to as-implanted specimens except the difference in the oxygen and nitrogen profiles. The profile of the alloying elements, iron, chromium, nickel, molybdenum, and titanium, showed the decrease in the intensity in the implanted region similar to that of the as-implanted specimen. The enrichment of nitrogen was observed in the few angstroms in the top surface layers of implanted-passivated specimens compared to the as-implanted specimen. In the oxygen profile, the as-implanted specimen showed the sharp decrease in intensity as it reached the steady state. It indicated that the high intensity of oxygen at the top layers arose from the passive film, and when it entered the bulk, the profile reached the steady state. However, in the case of the implanted-passivated specimen, it showed the least intensity at the initial stage. Then it increased gradually and reached the maximum within a few angstroms, and then it fell rapidly to the steady state. This indicated that at the top layers of the passive film, concentration of oxygen was low, and it increased in the inner layer of the passive film. The changes in the oxygen profile for the implanted-passivated specimen indicated that the outer surface of the passive film was mainly predominated by nitrogen, which prevented the corrosion resistance. In the case of the unimplanted-passivated specimen, the oxygen profile was very similar to the as-implanted specimen. All of these suggest that during passivation of the implanted specimen, the

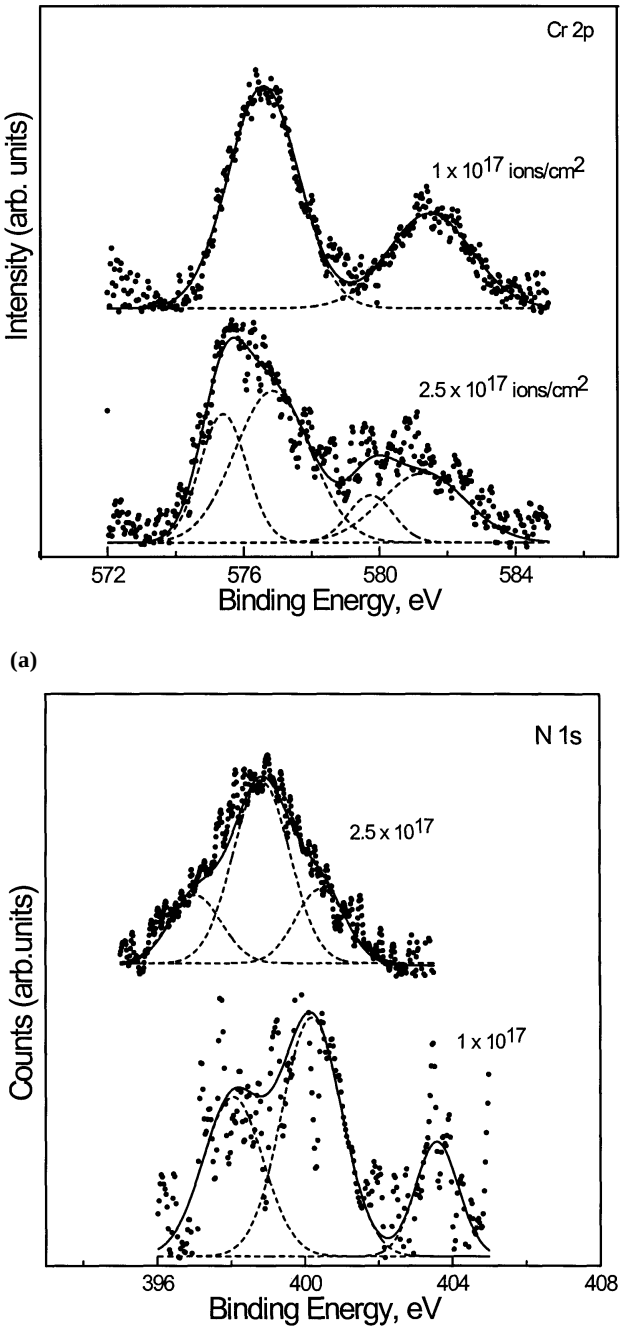

Fig. 7 X-ray photoelectron spectroscopy of (a) Cr 2p and (b) N 1s spectra for implanted-passivated titanium-modified type 316L SS specimens

alloying elements would have converted into their oxide and simultaneously dissolved the alloying elements into the solution, leaving the nitrogen at the surface. At one stage, dissolution of these alloying elements became slow due to the increase in the concentration of nitrogen at the surface, blocking the further attack of the aggressive chloride ions. It resulted in the enrichment of nitrogen and depletion of oxygen observed at the surface. The enrichment of nitrogen at the surface inhibited the oxide species from approaching the metal constituent for further oxide growth. This can be confirmed from the depth profiles of chromium, iron, nickel, and molybdenum, which showed the low intensity at the near surface region (passive film).

Osazawa and Okato (Ref 32) suggested the improved pitting resistance of nitrogen added stainless steels to the formation of NH_4^+ at the pit site by consuming the excess H~+ produced by an autocatalytic reaction. The formation of NH_4^+ increased the pH at the pit site and slowed down the pit propa-

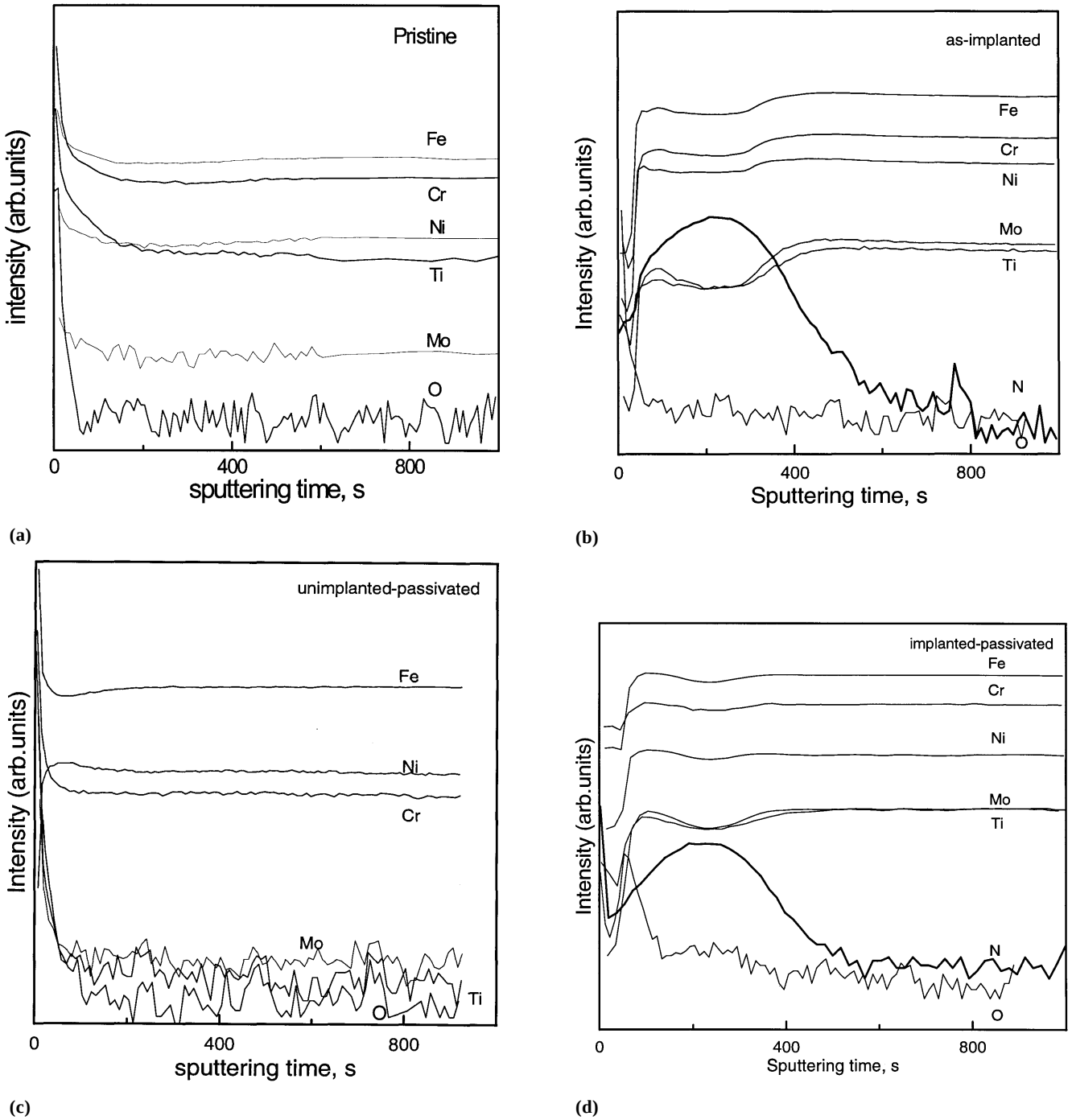

Fig. 8 Secondary ion mass spectroscopy depth profile for (a) pristine, (b) as-implanted, (c) unimplanted-passivated, and (d) implanted-passivated, titanium-modified type 316L SS specimens

gation. During the active dissolution and initial stages of passivation, alloying elements such as iron, chromium, and nickel dissolved in the electrolyte, whereas nonactive elements such as nitrogen remained on the surface, leading to the enrichment in nitrogen. The enrichment of nitrogen was nearly seven times that of initial nitrogen composition of the alloy (Ref 33-34). Newman and Shahrabi (Ref 35) suggested that the enrichment of nitrogen on the surface of the passive film will prevent the dissolution of the alloying elements by blocking some of the kink sites. Kamachi Mudali et al. (Ref 36) reported that the formation of ammonium ions at the pit site formed subsequently, inhibiting nitrate compounds. Misawa and Tanabe (Ref 37) substantiated this hypothesis by observing the nitrate species in the pit precursor region of high nitrogen austenitic stainless steel. The increase in the pitting potential of nitrogen ion implanted titanium-modified SS was attributed to the formation of NH_4^+ and subsequently transformed into nitrates. X-ray photoelectron spectroscopy N 1s spectra for high dose specimen also showed that the peak at 403.5 eV corresponded to nitrates. Also, the passive current density of the N^+ implanted specimens considerably decreased as the nitrogen content increased up to the dose 1×10^{17} ions/cm^2. Secondary ion mass spectroscopy results showed the enrichment of nitrogen at the surface along with the depletion of the alloying elements. X-ray photoelectron spectroscopy studies showed the major amount of nitrogen present in the surface of the passive film exists as oxynitrides. This reveals that the formation of an enriched nitrogen layer prevents the further attack of aggressive chloride ions.

4. Conclusions

The present investigation shows:

- Addition of titanium in the 316L SS increased the localized corrosion resistance in the Ringer's solution. This beneficial effect was attributed to the presence of titanium in the passive film.
- Nitrogen ion implantation improved the localized corrosion resistance of titanium modified type 316L SS. The implanted specimens showed variations in the corrosion resistance with varying doses, and the specimen implanted at 1×10^{17} ions/cm^2 showed an optimum corrosion resistance.
- The detrimental effect of the specimen implanted at the dose of 2.5 x 10^{17} ions/cm^2 was attributed to the formation of nitrides during implantation, which creates the inhomogeneities in the passive film.
- The enhanced localized corrosion resistance of nitrogen ion implanted titanium-modified 316L SS was attributed to the protective oxynitrides formation in the passive film, and formation of nitrates at the pit site inhibited the pit propagation and widened the passive range of titanium-modified type 316L SS.

Acknowledgments

The authors are very thankful to Dr. R.K. Dayal, Head, ACSSS, M.D. and Dr. V.S. Raghunathan, Head, M.D. of IGCAR for their interest in this work. Dr. S. Rajagopalan, MSD, IGCAR is gratefully acknowledged for assistance with the SIMS experiments. T. Sundararajan also acknowledges IUC-DAEF, Indore for financial assistance.

References

1. O.E.M. Pohler, *Failure and Prevention,* Vol 11, *Metals Handbook,* 9th ed., K. Mills, Ed., American Society for Metals, 1986, p 670
2. K. Nielsen, *Br. Corros. J.,* Vol 22, 1987, p 272
3. M. Sivakumar, U. Kamachi Mudali, and S. Rajeswari, *J. Mater. Eng. Perform.*, Vol 3, 1994, p 744
4. M. Sivakumar and S. Rajeswari, *J. Mater. Sci. Lett.*, Vol 11, 1992, p 1039
5. M. Sivakumar, U. Kamachi Mudali, and S. Rajeswari, *Steel Research,* Vol 65, 1994, p 76
6. M. Sivakumar, U. Kamachi Mudali, and S. Rajeswari, *Proceedings of the Twelfth International Corrosion Congress,* Vol 3B, 1993, p 1942
7. V. Ashworth, W.A. Grant, and R.P.M. Procter, *Corros. Sci.,* Vol 16, 1976, p 661
8. E. McCafferty, P.G. Moore, J.D. Ayers, and G.K. Hubler, Corrosion of Metal Processed by Directed Energy Beams, C.R. Clayton and C.M. Preece, Ed., The Metallurgical Society AIME, New York, 1982, p 1
9. J. Jedrkowski, J. Martan, J. Masalski, and D.B. Bogomolov, *Phys. Stat. Solid,* Vol A, 1989, p 112
10. J.E. Trueman, M.J. Coleman, and K.R. Pirt, *Brit. Corros. J.,*. Vol 12, 1977, p 236
11. U. Kamachi Mudali, R.K. Dayal, J.B. Gnanamoorthy, and P. Rodriguez, *Mater. Trans. JIM,* Vol 37, 1996, p 1568
12. R. Sabot, R. Devaux, A.M. de Becdelievre, and C. Duret-Thual, *Corros. Sci.,* Vol 33, 1992, p 1121
13. P. Marcus and M.E. Bussell, *Appl. Surf. Sci.,* Vol 59, 1992, p 7
14. M.R. Nair, S. Venkatraman, D.C. Kothari, K.B. Lal, and R. Raman, *Nucl. Instr. Meth. in Phys. Res.,* Vol B34, 1988, p 53
15. E. Leito, R.A. Silva, and M.A. Barbosa, *J. Mater. Sci.: Mater. Med.*, Vol 8, 1997, p 365
16. I. Bertoti, M. Mohai, J.L. Sullivan, and S.O. Saied, *Appl. Surf. Sci.,* Vol 84, 1995, p 357
17. U. Kamachi Mudali, R.K. Dayal, S. Venkadesan, and J.B. Gnanamoorthy, *Met. Mater. Proc.*, Vol 8, 1996, p 139
18. N.D. Tomashov, G.P. Charnova, and O.N. Marcova, *Corrosion,* Vol 20, 1964, p 166
19. Sydberger, *Werkst. Korros.,* Vol 32, 1981, p 179
20. H.H. Strehblow, *Werkst. Korros.,* Vol 35, 1984, p 437
21. A. Cerquetti, F. Mazza, and M. Vigano, *Corrosion—NACE-3,* R.N. Stachle, B.F. Brown, J. Kruger, and A. Agrawal, Ed., NACE, Texas, 1974, p 644
22. D.F. Williams, *J. Mater. Sci.,* Vol 22, 1987, p 3421
23. U. Kamachi Mudali, T. Sundararajan, K.G.M. Nair, and R.K. Dayal, Proceeding of the International Conference on Corrosion, CORCON-97, NACE, *Corrosion and Its Control,* A.S. Khanna, M.K. Totlani, and S.K. Singh, Ed., Elsevier, Vol 2, 1997, p 566
24. U. Kamachi Mudali, T. Sundararajan, K.G.M. Nair, and R.K. Dayal, " Pitting and Intergranular Corrosion Resistance of Nitrogen Ion Implanted Type 304 Stainless Steel," presented at High Nitrogen Steels (Espoo, Finland), HNS-98, May 1998
25. R.G. Vardiman and I.L. Singer,Pitting and Intergranular Corrosion Resistance of Nitrogen Ion Implanted Type 304 Stainless Steel, *Mater. Lett.*, Vol 2, 1983, p 150
26. J.L. Whitton et al., *Mater. Sci. Eng.,* Vol 69, 1985, p 111
27. R. Leutenecker, G. Wagner, T. Louis, V. Gonser, L. Guzman, and A. Molinari, *Mater. Sci. Eng.,* Vol A115, 1989, p 229
28. C.D. Wagner, W.M. Riggs, L.E. Davis, J.F. Moulder, and G.E. Muilenberg, Ed., *Handbook of XPS,* Perkin-Elmeir Corp., 1980

29. J.S. Murday and I.L. Singer, *J. Vac. Sci. Technol.*, Vol 17, 1980, p 327
30. A. Sadough Vanini, J.P. Audouard, and P. Marcus, *Corr. Sci.*, Vol 36, 1994, p 1825
31. V. Ashworth, W.A. Grant, R.P.M. Procter, and T.C. Wellinton, *Corr. Sci.*, Vol 16, 1976, p 396
32. K. Osazawa and N. Okato, *Effect of Alloying Elements, Especially Nitrogen, on the Initiation of Pitting in Stainless Steel, Passivity, and Breakdown on Iron and Iron Base Alloys*, R. Stachle and H. Okado, Ed., NACE, Texas, 1976, p 135
33. Y.C. Lu, R. Bandy, C.R. Clayton, and R.C. Newman, *J. Electrochem. Soc.*, Vol 130, 1983, p 1175
34. R.C. Newman, Y.C. Lu, R. Bandy, and C.R. Clayton, *Proc. of Ninth Intern. Congress on Metallic Corrosion*, Vol 1, National Research Council, 1984, p 394
35. R.C. Newman and T. Shahrabi, Vol 27, 1987, p 827
36. U. Kamachi Mudali, T.P.S. Gill, R.K. Dayal, and J.B. Gnanamoorthy, *Werks. Korros.*, Vol 37, 1986, p 637
37. T. Misawa and H. Tanabe, *ISIJ International*, Vol 36, 1996, p 821